

SYMBOLIC TRANSFER ENTROPY REVEALS THE AGE STRUCTURE OF PANDEMIC INFLUENZA TRANSMISSION FROM HIGH-VOLUME INFLUENZA-LIKE ILLNESS DATA

STEPHEN M KISSLER^{1,2}, CÉCILE VIBOUD³, BRYAN T GRENFELL⁴, JULIA R GOG¹

¹*Department of Applied Mathematics and Theoretical Physics, University of Cambridge, Wilberforce Road, Cambridge, United Kingdom*

²*Department of Immunology and Infectious Diseases, Harvard T.H. Chan School of Public Health, Boston, Massachusetts, United States of America*

³*Fogarty International Center, National Institutes of Health, Bethesda, Maryland, United States of America*

⁴*Department of Ecology and Evolutionary Biology, University of Princeton, Princeton, New Jersey, United States of America*

ABSTRACT. Existing methods to infer the relative roles of age groups in epidemic transmission can normally only accommodate a few age classes, and/or require data that are highly specific for the disease being studied. Here, symbolic transfer entropy (STE), a measure developed to identify asymmetric transfer of information between stochastic processes, is presented as a way to determine which age groups drive an epidemic. STE provides a ranking of which age groups dominate transmission, rather than a reconstruction of the explicit between-age-group transmission matrix. Using simulations, we establish that STE can identify which age groups dominate transmission, even when there are differences in reporting rates between age groups and even if the data is noisy. Then, the pairwise STE is calculated between time series of influenza-like illness for 12 age groups in 884 US cities during the autumn of 2009. Elevated STE from 5-19 year-olds indicates that school-aged children were the most important transmitters of infection during the autumn wave of the 2009 pandemic in the US. The results may be partially confounded by higher rates of physician-seeking behaviour in children compared to adults, but it is unlikely that differences in reporting rates can explain the observed differences in STE.

KEYWORDS: Symbolic transfer entropy; pandemic influenza; age structure; electronic medical records; influenza-like illness

1. INTRODUCTION

Age is a key predictor of a person's rate of both acquiring [1, 2, 3, 4, 5, 6] and transmitting [7, 8, 9] influenza. Children tend to contribute more to influenza transmission than adults do [4, 7, 8], but the precise epidemiological roles of different age groups can shift from season to season [10] and may change markedly in pandemic years [11]. From a public health perspective, untangling the relative roles of different age groups could help guide targeted vaccination strategies [7, 12, 13, 14]

7 and other age-related interventions, like the selective closure of schools [15, 16, 17]. However,
8 data with sufficient resolution to identify detailed epidemiological relationships between age groups
9 has so far been scarce, and even when such data exist, current methods are insufficient for reliably
10 uncovering those relationships.

11 Electronic medical records (EMRs) help address the issue of data scarcity by providing high-
12 volume influenza-like illness (ILI) incidence data with detailed age structure [18]. EMRs are rou-
13 tinely produced by physicians for insurance purposes during the majority of outpatient visits in the
14 United States [18]. Since EMRs generally contain syndromic illness classifications, EMR-based
15 estimates of influenza incidence are subject to noise from non-ILI respiratory infection. EMR-
16 based disease incidence estimates are also subject to geographic and demographic variation in
17 physician-seeking behaviour. Laboratory-confirmed influenza cases, as collected routinely by the
18 Centers for Disease Control and Prevention (CDC) [19], provide more specific estimates of in-
19 fluenza incidence, but at substantially lower volume. Influenza incidence estimates from online
20 search platforms and social media websites like Google [20] and Twitter [21] can provide massive
21 amounts of data, but these sources' reliability has been called into question, and they lack detailed
22 age information [22]. Dedicated online platforms such as FluNearYou in the US and FluSurvey in
23 the UK, which gather reports of ILI symptoms from community volunteers [23, 24], hold some
24 promise for supplementing traditional ILI data streams [25, 26, 27], but represent a relatively small
25 convenience sample of the population. So, while other data sources exist, EMRs offer a relatively
26 promising and so-far underutilised source of fine-scale data on influenza incidence in the United
27 States [18, 22].

28 Previous attempts to infer the relative importance of different age groups for the transmission of
29 influenza have sought to either reconstruct the explicit next-generation matrix (NGM) [3, 28, 29]
30 or to infer the relative risk of infection between age groups [4]. The NGM-based methods have
31 only been applied to scenarios with at most two age groups (children and adults), in part because
32 they require strong assumptions about the structure of the next-generation matrix which become
33 increasingly unrealistic as the number of age classes grows. The relative risk method [4] has been
34 used to rank the importance of five age groups for the transmission of influenza, but requires data
35 with high specificity for influenza, effectively precluding ILI datastreams and the use of EMRs in
36 particular.

37 Symbolic transfer entropy (STE) [30] offers a way to infer the relative transmissive importance of
38 possibly many age groups from ILI data. STE is an extension of transfer entropy (TE) [31], which
39 measures the amount of information the past states of one stochastic process provide about the
40 transition probabilities of another. Intuitively, the TE is a measure of the amount of information
41 “transferred” from one stochastic process to another. To compute the STE, a time series is sym-
42 bolised using a scheme that encodes its qualitative structure in a low-dimensional space, and then
43 the TE is calculated from the relative frequencies of these symbols. The symbolisation scheme
44 makes the STE robust to minor point-wise noise and to systematic shifts in amplitude, which in the
45 context of EMR ILI data might arise from the presence of non-influenza ILI cases and from differ-
46 ences in reporting rate between age groups. These benefits come with the trade-off of requiring
47 relatively large amounts of data compared to existing methods for inferring the age structure of
48 disease transmission. STE has been used to study epileptogenic neural signals and the dis-
49 semination of information through social networks [30, 32], but to our knowledge has not been
50 systematically evaluated as a means of providing insight into infectious disease transmission. TE
51 and STE are similar to other model-free methods that measure shared information and so-called
52 ‘causal’ relationships between stochastic processes, including mutual information [31], Granger
53 causality [33], and convergent cross mapping [34]. Permutation entropy, a related measure, has
54 recently been used to quantify the predictability of infectious disease outbreaks [35].

55 Here, we use influenza-like outbreak simulations to demonstrate that STE reliably identifies the
56 age groups that drive influenza transmission. Then, we utilise an EMR-based dataset capturing
57 ILI incidence from 884 ZIP (postal) codes and 12 age classes across the United States to rank
58 the relative importance of the various age groups in the transmission of the autumn wave of the
59 2009 A/H1N1pdm influenza pandemic in that country. We conclude that school-aged children
60 (5–19 year-olds) were disproportionately responsible for transmitting influenza to infants through
61 working-age adults in the autumn of 2009, in broad agreement with other findings. Our work
62 demonstrates that STE could serve as an important tool for the detailed epidemiological analysis
63 of age structure, especially as EMR data become more prevalent.

64

2. MATERIALS AND METHODS

65 2.1. **Data.** The data come from a convenience sample of CMS-1500 electronic medical claims
66 forms submitted by primary care physicians across the US and maintained by SDI health (now

67 IQVIA). Each claim is associated with a single outpatient visit, and includes one or more ICD-9
68 codes [36] listed by the physician that describe the patient's illness. The overall sample is thought
69 to capture over 50% of all outpatient visits in the US in 2009 [18]. The records are binned weekly
70 and aggregated geographically by the first three digits of the ZIP (postal) code of the practice from
71 which they are submitted [37]. These three-digit ZIP codes will be referred to simply as 'ZIPs' (not
72 to be confused with the finer five- or ten-digit ZIP codes, also assigned to many mailing addresses
73 in the US [36]). Time series of weekly influenza-like illness (ILI) incidence are created by extracting
74 claims with a direct mention of influenza, or fever combined with a respiratory symptom, or febrile
75 viral illness (ICD-9 487-488 OR [780.6 and (462 or 786.2)] OR 079.99), following Viboud *et al.*
76 (2014) [18]. For each ZIP, the number of ILI cases in each week is divided by the total number
77 of patients who visited a physician in that ZIP during that week, yielding an 'ILI ratio' time series.
78 There are 884 ILI ratio time series, one for each ZIP in the lower 48 US states, each spanning
79 52 weeks from the week commencing 4 Jan 2009 through the week commencing 27 Dec 2009.
80 The correspondence between the SDI-ILI dataset and reference influenza surveillance data from
81 the US Centers for Disease Control and Prevention (CDC) is described in depth by Viboud *et al.*
82 (2014) [18].

83 **2.2. Symbolic transfer entropy.** If I and J are discrete-state and discrete-time random pro-
84 cesses such that i_t and j_t are the states of processes I and J at time t , then the transfer entropy
85 (TE) from process J to process I is defined as

$$(1) \quad T_{J \rightarrow I} = \sum_{\Omega_I, \Omega_J} p(i_{t+1}, i_t^{(k)}, j_t^{(l)}) \log \left(\frac{p(i_{t+1} | i_t^{(k)}, j_t^{(l)})}{p(i_{t+1} | i_t^{(k)})} \right)$$

86 where $i_t^{(k)}$ is shorthand notation for the k -step history of process i , (i_t, \dots, i_{t-k+1}) , and similarly
87 $j_t^{(l)} = (j_t, \dots, j_{t-l+1})$. The logarithm has base 2, so that the transfer entropy is measured in
88 bits. The sum is over all possible combinations of states $(i_{t+1}, i_t^{(k)}, j_t^{(l)})$, where $i_{t+1}, i_t^{(k)} \in \Omega_I$ and
89 $j_t^{(l)} \in \Omega_J$, and Ω_I and Ω_J are the state spaces for processes I and J . Eq. 1 is a Kullback-Leibler
90 divergence that measures how much process I deviates from the generalised Markov property
91 $p(i_{t+1} | i_t, \dots, i_1) = p(i_{t+1} | i_t^{(k)})$, given the last l states of process J . In practice, the histories are
92 often fixed at length 1 ($k = l = 1$) and the probabilities are estimated from simple counts of the
93 observed data [31].

94 The TE is limited in that it is only defined for stochastic processes with a discrete state space.
95 Staniek and Lehnertz (2008) [30] introduce symbolic transfer entropy (STE) as a way to calculate
96 information transfer between time series processes that have continuous- or near-continuous state
97 spaces. Motivated by the insight that the relative amplitudes of subsequent observations from
98 these sorts of processes may provide enough information to reveal interactions between them,
99 they propose symbolising the time series based on ordered m -tuples of observations (Fig. S1).
100 This reduces the (near-)continuous state space of the original stochastic process to a discrete set
101 of $m!$ symbols. In practice, m is often chosen to be 2 or 3, giving a state space of 2 or 6 symbols,
102 respectively. For $m = 3$, we also tested the effect of collapsing the two concave-up and the two
103 concave-down symbols into a single symbol each, resulting in a smaller state space (four vs. six
104 symbols) while capturing a similar level of qualitative detail. Details on the symbolisation of time
105 series and the empirical calculation of the STE are provided in the Supplemental Information.

106 **2.3. SIR epidemic simulation model.** For simulations with just two age classes, we use a sto-
107 chastic SIR model implemented using the Gillespie algorithm [38]. For all simulations, the basic
108 reproduction number R_0 is set at 1.5, consistent with estimates of the basic reproduction number
109 of 2009 A/H1N1 pandemic influenza [39, 40]. We consider a population size of $N = 1,000$ split
110 evenly between classes 1 and 2, so that $N_1 = N_2 = 500$ (age groups with different population
111 sizes are also considered in the Supplemental Information). The expected time to recovery $1/\gamma$ is
112 assumed constant for all age groups and is set at 7 days, which is consistent with estimates of the
113 infectious period for 2009 pandemic influenza [40]. Table S1 gives the rates at which individuals of
114 each class stochastically progress from susceptible to infected to recovered. Infections are binned
115 into week-long intervals, and Poisson noise is added to simulate non-influenza influenza-like ill-
116 ness. Fig. S7 depicts five incidence time series produced using the model. Full details on the
117 model and simulation procedure are given in the Supplemental Information.

118 **2.4. Poisson epidemic simulation model.** For more than two age classes, the full stochastic
119 SIR model becomes too computationally demanding for repeated simulations to be practical. So,
120 we also define an outbreak simulation model based on a self-exciting Poisson process, similar to
121 [41]. We choose the time units t to match the mean generation interval of the infection, which we
122 set at 3.5 days [42]. To generate epidemics, we use a stepwise-constant effective reproduction
123 number R_t , such that $R_t = 1.5$ for the first four weeks (eight generations) of the outbreak and

124 $R_t = 0.8$ thereafter. Infections are binned from the half-week generations into week-long intervals,
125 and additional Poisson noise is added to each bin to simulate non-influenza influenza-like illness.
126 For simulations with two age classes, the Poisson model yields epidemics of similar length and
127 magnitude as the two-age-class SIR model (compare Figs S7 and S8), and yields comparable STE
128 inferences (see Fig. 1), which suggests that the Poisson model is an acceptable approximation to
129 the stochastic SIR model. Full details on the implementation of the Poisson model are given in the
130 Supplemental Information.

131 **2.5. Reporting rates.** Only a fraction of influenza cases are represented in the SDI-ILI dataset,
132 since many people do not seek medical care for their symptoms. The tendency to seek medical
133 care given infection with an ILI can vary by age group [43]. To factor this into the outbreak simula-
134 tions, we introduce a reporting rate vector c in which element c_i gives the expected proportion of
135 individuals in age class i who seek medical care when infected with an ILI. It is then possible to
136 simulate a ‘reported’ disease incidence time series:

$$(2) \quad Y_{i,t}^{obs} \sim Binomial(Y_{i,t}, c_i)$$

137 where $Y_{i,t}$ is the simulated number of infected individuals in age class i at time t (under either
138 model) and $Y_{i,t}^{obs}$ is the simulated reported number of infections in age class i at time t .

3. RESULTS

140 **3.1. STE reveals transmission asymmetries between two coupled age groups.** We first cal-
141 culate the STE between two age groups as the within- and between-group reproduction ratios
142 vary. We consider between-group transmission that ranges from (a) fully decoupled to fully sym-
143 metric, and (b) fully symmetric to strongly driven by Group 1. The between-group infectiousness is
144 specified using a “relative reproduction matrix” r , which is a scaled version of the next-generation
145 matrix [28], such that $r_{i,j}/r_{k,j}$ gives the proportional difference in group j ’s infectiousness for
146 group i vs. group j . For example, if $r_{i,j}/r_{k,j} = 2$, then a member of group j is expected to infect
147 twice as many members of group i than of group k . Scenario (a) is encapsulated by the relative
148 reproduction matrix

$$(3) \quad \mathbf{r}_a = \begin{bmatrix} 1 & z_a \\ z_a & 1 \end{bmatrix}$$

149 where $z_a \in [0, 1]$. Scenario (b) is encapsulated by the relative reproduction matrix

$$(4) \quad \mathbf{r}_b = \begin{bmatrix} 1 + 3z_b & 1 \\ 1 + z_b & 1 \end{bmatrix}$$

150 where $z_b \in [0, 1]$.

151 Fig. 1 depicts the change in STE under these two transmission scenarios, calculated from
152 epidemics simulated using the stochastic SIR model (Fig. 1 A–B) and the Poisson model (Fig. 1
153 C–D). Each pane in Fig. 1 is produced using 100 ensembles of 800 simulated epidemics for each
154 value of z_a and z_b between 0 and 1 in steps of size 0.1. For each ensemble, the 800 simulated
155 incidence time series are symbolised using symbols of length $m = 3$, and then the between-group
156 transfer entropies are estimated using the relative symbol frequencies (see Fig. S3), producing 100
157 STE estimates for each value of z_a and z_b . The solid blue (black) lines in Fig. 1 depict the mean
158 Group 1→2 (Group 2→1) STE for each value of z_a and z_b across the 100 ensembles. The shaded
159 blue (black) bands depict the range of the middle 95 Group 1→2 (Group 2→1) STE estimates for
160 each value of z_a and z_b across the 100 ensembles, analogous to a 95% confidence interval. Under
161 both the stochastic SIR and the Poisson models, the between-group STE increases steadily as
162 the transmissive coupling ranges from none to symmetric (Fig. 1 A, C). Once Group 1 begins to
163 dominate transmission, the Group 1→2 STE increases and the Group 2→1 STE decreases (Fig.
164 1 B, D), accurately capturing the transmissive relationship between the age groups.

165 When Group 1 drives transmission, the Poisson model yields a smaller difference in the STE
166 between the two age groups than the stochastic SIR model does (Fig. 1 B, D). Visual inspection
167 suggests that the simulated time series produced using the stochastic SIR model tend to feature
168 more stochastic fluctuations than the time series produced using the Poisson model (Figs S7 and
169 S8). Since STE is effectively a measure of how these stochastic fluctuations transmit from one
170 age group to another, this may explain why the differences in STE calculated using the Poisson
171 model are relatively less pronounced. Overall, the qualitative similarity between the STE estimates

172 from the two transmission models suggests that the Poisson model is an acceptable approxima-
173 tion to the stochastic SIR model, and that simulations from the Poisson model tend to produce
174 more conservative estimates of the difference in STE between age groups than the stochastic SIR
175 model.

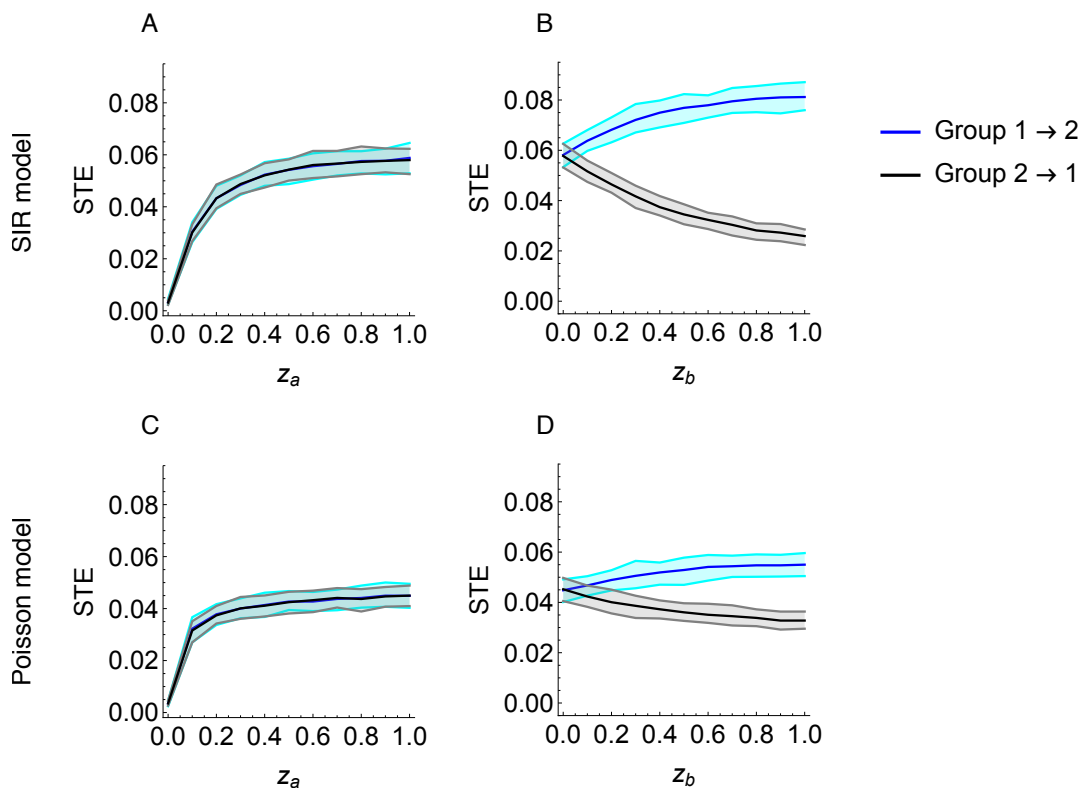


FIGURE 1. Mean (95% CI) Group 1→2 (blue) and Group 2→1 (black) STE values as the coupling between the two groups ranges from none to fully symmetric (A and C), and from fully symmetric to strongly driven by Group 1 (B and D). The curves are produced by simulating 100 ensembles of 800 epidemics each from the stochastic SIR model (A and B) or the Poisson model (C and D) for each value of z_a and z_b between 0 and 1 in steps of 0.1, and then calculating the between-group STE for each ensemble. The relative reproduction matrices that capture these two coupling scenarios are given in Eqs 3 and 4.

176 **3.2. STE reveals transmission asymmetries despite incomplete reporting.** Next, we evaluate
177 how incomplete reporting influences the detection of asymmetries in transmission strength. Fig.
178 2 depicts the mean estimated STE across 100 ensembles of 800 epidemics each for reporting
179 rates c_i between 0.1 and 1 in steps of 0.1, with equal reporting rates across all age groups. The
180 epidemic simulations are produced using the Poisson model with relative reproduction matrix

$$(5) \quad r = \begin{bmatrix} 1 & 2 & 1 & 1 \\ 1 & 4 & 1 & 1 \\ 1 & 2 & 1 & 1 \\ 1 & 1 & 1 & 1 \end{bmatrix}$$

181 which could represent ‘children’ (Group 2) having strong within-group transmission ($r_{2,2} = 4$) and
182 intermediate transmission to ‘infants’ (Group 1) and ‘adults’ (Group 3) ($r_{1,2} = r_{3,2} = 2$). Even for
183 reporting rates as low as 0.1, the STE values from Group 2 are higher than those from any other
184 group. As the reporting rates increase, the differences become more pronounced, accurately
185 capturing the transmissive dominance of Group 2 over the other groups. The estimated STE
186 increases with reporting rate for all age groups, but more quickly for Group 2 than for the other
187 age groups. According to Biggerstaff *et al.* (2012) [43], true reporting rates for ILI in the US during
188 the 2009 pandemic were between 0.4 and 0.6, for which the transmissive dominance of Group 2
189 is clear.

190 **3.3. STE reveals transmission asymmetries between twelve coupled age groups.** To test the
191 ability of STE to identify transmission asymmetries from data on the scale of the SDI-ILI dataset,
192 we use the Poisson model to simulate 100 ensembles of 800 epidemics each with 12 age groups.
193 We consider the scenarios (a) with the 12×12 relative reproduction matrix Eq. S48, representing
194 high transmission from Groups 3–5 to Groups 3–5 ($r_{i,j} = 4$ for $i, j \in \{3, 4, 5\}$), intermediate
195 transmission from groups 3–5 to groups 1–2 and 6–9 ($r_{i,j} = 2$ for $i \in \{1, 2, 6, 7, 8, 9\}$ and $j \in$
196 $\{3, 4, 5\}$), baseline transmission ($r_{i,j} = 1$) between all other groups, and uniform 50% reporting
197 rate across all groups, and (b) with uniform transmission strength across all age groups (i.e. a
198 12×12 relative reproduction matrix with ‘1’ for all entries), 60% reporting rate for groups 1–5, and
199 40% reporting rate for groups 6–12, following the estimates of Biggerstaff *et al.* (2012) [43] for the
200 ILI reporting rates in the United States during the 2009 influenza pandemic for children and adults,
201 respectively.

202 Fig. 3 depicts the mean pairwise STE estimates between the 12 age groups under both sce-
203 narios. The square in row i and column j represents the STE from Group j to Group i . Darker
204 squares correspond to higher STE. For the asymmetric transmission/uniform reporting rate sce-
205 nario (scenario (a), Fig. 3A), the STE clearly captures the transmissive dominance of Groups 3,

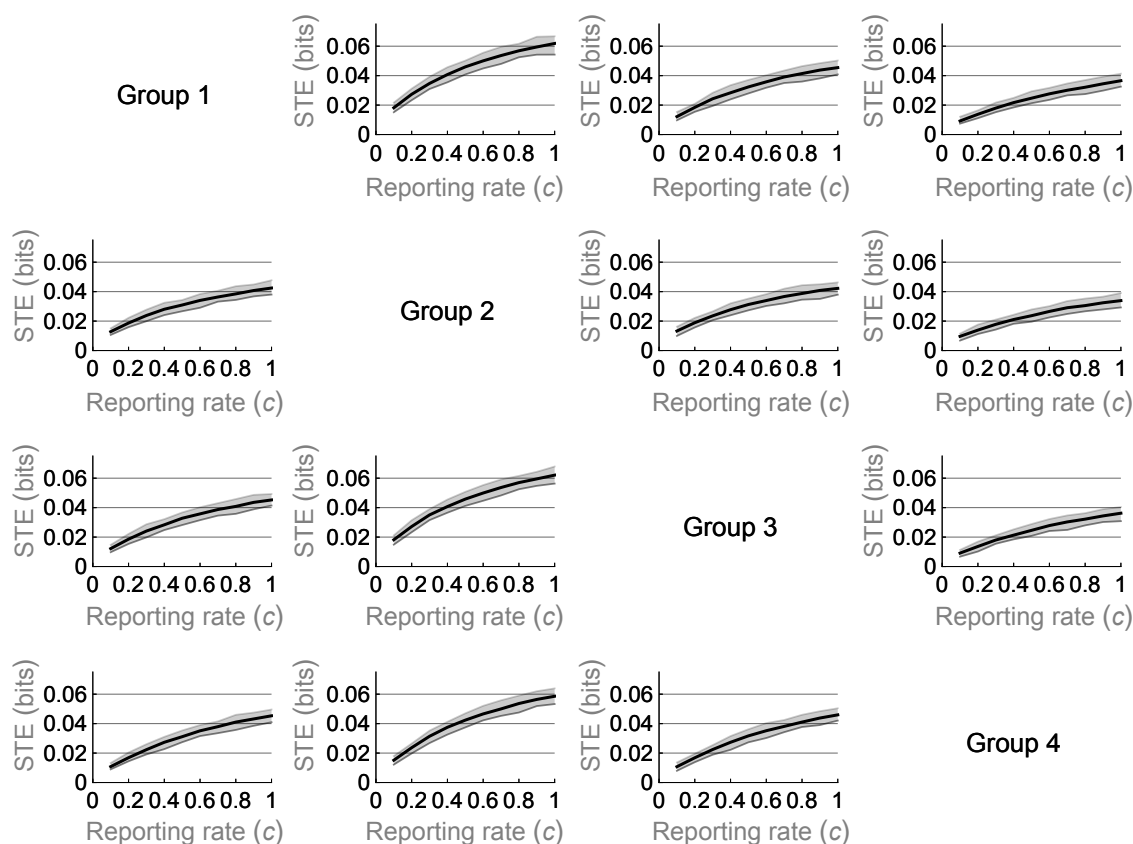


FIGURE 2. Mean pairwise STE values (solid lines) with 95% confidence intervals (shaded bands) for epidemics strongly driven by Group 2 under a range of reporting rates c . The curves are produced by simulating 100 ensembles of 800 epidemics each from the Poisson model for each value of c between 0.1 and 1 in steps of 0.1, and then calculating the between-group STE for each ensemble. The reporting rate c_i (see Eq. 2) is varied uniformly across all age groups i . The relative reproduction matrix that specifies within- and between-group transmission rates is given by Eq. 5. The plot in row i and column j depicts the STE from group j to group i .

206 4, and 5. The pairwise STE does not simply reproduce the structure of the relative reproduction
 207 matrix, as evidenced by the variability in mean pairwise STE for age groups other than Groups
 208 3–5. This is because the STE captures a ‘knock-on’ effect for which information transferred from
 209 a strongly-driving age group can propagate through other age groups. For the uniform transmis-
 210 sion/variable reporting rate scenario (scenario (b), Fig. 3B), it is evident that elevated reporting
 211 rates can also lead to elevated STE, both to and from the groups with elevated reporting rate
 212 (Groups 1–5). Overall, the variability in STE due to differences in reporting rate appears to be
 213 smaller than the variability in STE due to differences in transmission strength. Further discussion
 214 on the effect of reporting rates on STE may be found in the Supplemental Information.

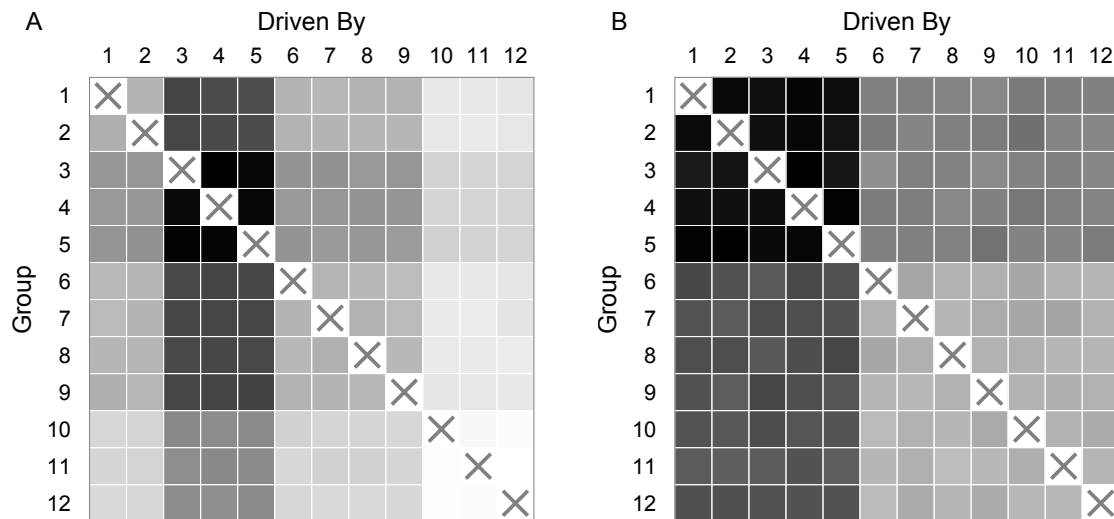


FIGURE 3. Mean pairwise STE values between 12 groups for epidemics strongly driven by Groups 3, 4, and 5 and uniform 50% reporting rate across all age groups (A), and for epidemics driven equally by all age groups, 60% reporting for Groups 1–5, and 40% reporting for Groups 6–12 (B). A box in row i and column j corresponds to the STE from group j to group i , where darker shades corresponds to higher STE. To generate the STE values, 100 ensembles of 800 epidemics were simulated from the Poisson model using relative rate matrix Eq. S48 for (A) or a relative rate matrix with all entries equal to 1 for (B). Each ensemble generates 144 pairwise STE values, so that each box represents the mean value across the 100 ensembles. The raw values are listed in Eqs S49 and S50.

215 **3.4. School-aged children contributed disproportionately to transmission during the au-**
 216 **tumn 2009 A/H1N1pdm influenza outbreak in the US.** To estimate the pairwise STE between
 217 the 12 age groups represented in the SDI-ILI dataset during the 2009 A/H1N1pdm influenza pan-
 218 demic, we extract data from the 25 weeks between 12 July 2009 and 27 December 2009 and
 219 symbolise the ILI time series for each age group in each ZIP using a symbol length of $m = 3$.
 220 The pairwise STE values between all age groups are depicted in Fig. 4. The STE is highest in
 221 the columns representing 5–19 year-olds. This provides evidence that there was systematically
 222 elevated transmission from school-aged children to infants through adults. The adult-adult STE
 223 is also moderately elevated, suggesting that adults may have played a relatively important role in
 224 transmitting the outbreak amongst themselves, though this could also be explained by elevated
 225 transmission from children alone. Compare, for example, to the left-hand plot in Fig 3: in that
 226 simulation, only transmission from children is elevated, but it causes a moderate elevation in the
 227 STE from adults and infants to the other age groups due to the knock-on effect.

228 As a control, we also calculated the pairwise STE between all age groups during 25 post-
229 pandemic weeks, from 10 January 2010 through 27 June 2010. For these months, there is no
230 apparent age structure in transmission (see Supplemental Information). We also calculated the
231 pairwise STE between age groups for six previous influenza seasons (see Supplemental Informa-
232 tion). For the 2009 pandemic, there is a higher maximum pairwise STE and greater variation
233 in the pairwise STEs than for any previous season. This could reflect differences in baseline ILI,
234 which was likely lower during the autumn 2009 pandemic wave than during the seasonal out-
235 breaks, due to the pandemic's earlier timing. A lower baseline ILI might have made pairwise dif-
236 ferences in STE easier to detect in 2009. However, the relatively higher and more heterogeneous
237 STE values in 2009 are also consistent with the hypothesis that school-aged children played a dis-
238 proportionately large role in the spread of the 2009 pandemic, as has been described elsewhere
239 [4].

240 It is unlikely that differences reporting rates alone can account for the elevated STE from 5–19
241 year-olds to the other age groups. The mean pairwise STE values computed from simulations
242 with uniform transmission rates and unequal reporting rates in Section 3.3 range from .0057 to
243 0.0084 (see Eq. S50), while the pairwise STE values computed from the SDI-ILI data range from
244 0.0056 to 0.084 (see Eq. S51), an order of magnitude larger. The mean pairwise STE values
245 computed from simulations with asymmetric transmission and uniform reporting rates Section 3.3
246 range from 0.0047 to 0.014 (see Eq. S49), closer to the range observed from the SDI-ILI data
247 but still somewhat smaller. This points towards a possible combined effect of strong transmissive
248 driving from children plus elevated reporting in children. In addition, re-calculating the pairwise
249 STE using probabilistic reconstructions of the pre-reporting SDI-ILI incidence time series (see
250 Supplemental Information) indicate that the observed transmissive dominance of 5–19 year-olds
251 persists even after adjusting for potential differences in reporting rate between children and adults.
252 Furthermore, Biggerstaff *et al.* (2012) [43] report that 0-4 year-olds had the highest reporting rates
253 for ILI in the United States in 2009, yet the STE from 0-4 year-olds is relatively low compared to
254 the other age groups. If reporting rates alone could explain the observed differences in STE, the
255 STE from infants should be at least as high as the STE from school-aged children.

256 It is also unlikely that the unequal partitions of the age groups can explain the observed pat-
257 terns in the pairwise STE. The age groups under 20 years are partitioned such that they span

258 fewer years, and thus contain fewer individuals, than the age groups above 20 years. Direct cal-
 259 culations and simulations (see Supplemental Information) indicate that, all else being equal, the
 260 out-going STE for a given group tends to increase as the group's population size increases rel-
 261 ative to the sizes of the other groups. If differences in the groups' population sizes were driving
 262 the observed pairwise STE values, we would expect the age groups over 20 years to appear to
 263 dominate transmission – which is the opposite of what we observe here.

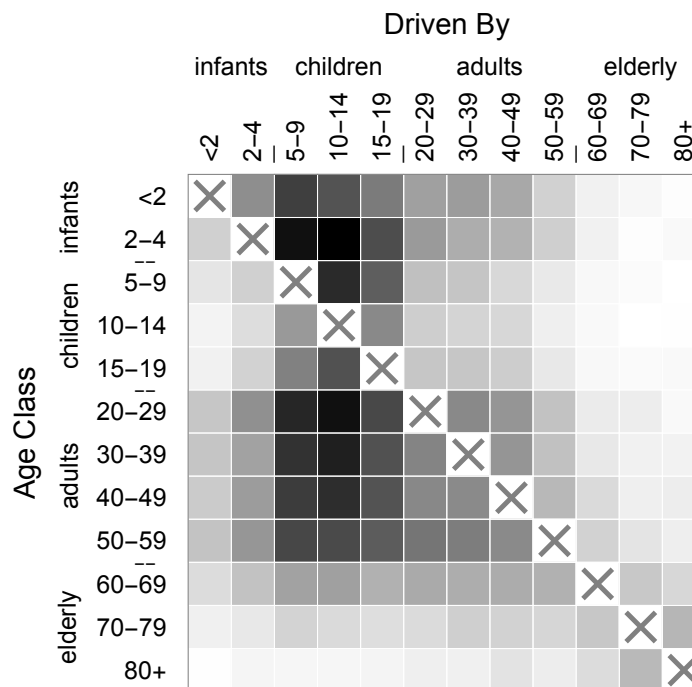


FIGURE 4. Mean pairwise STE values between the 12 groups represented in the SDI-ILI dataset during the autumn 2009 A/H1N1pdm pandemic influenza outbreak. A box in row i and column j corresponds to the STE from group j to group i , where darker shades corresponds to higher STE. The raw values are listed in Eq. S51.

264

4. DISCUSSION

265 Here, we propose STE as a means of ranking which age groups contribute most to the trans-
 266 mission of infectious disease outbreaks. STE is chosen for its robustness to point-wise noise
 267 and overall amplitude shifts in time series, which especially affect the ILI data stream due to non-
 268 influenza respiratory illness and incomplete reporting. Simulation studies indicate that STE can
 269 correctly rank transmissive asymmetries between age groups. However, STE is also positively as-
 270 sociated with reporting rates, which can partially confound estimates of asymmetric transmission.

271 STE estimates from ILI time series data from July-December 2009 in the United States suggest
272 that 5–19 year-olds were primarily responsible for driving transmission of the autumn wave of
273 the A/H1N1pdm pandemic influenza outbreak. It is unlikely that this result can be explained by
274 differences in reporting rates alone.

275 The identification of school-aged children as the primary drivers of transmission of the 2009
276 influenza pandemic in the United States agrees with most other studies on age-specific transmis-
277 sion of both seasonal and pandemic influenza [4, 7, 8, 9]. Elevated transmission from school-aged
278 children is likely due in part to the relatively high number of daily interpersonal contacts made by
279 members of these age groups. Mossong *et al.* (2008) [8] for example estimate that 10–19 year-
280 olds have more contacts per day than any other age group, and conclude from a modelling study
281 based on empirical contact data that 5–19 year-olds are likely to both suffer the highest burden of
282 disease and to drive the early-stage transmission of an outbreak transmitted by droplets through
283 close contacts, like influenza. This underscores the importance of monitoring children during pan-
284 demic influenza outbreaks, and potentially prioritizing school-aged children for vaccination.

285 TE is closely linked to mutual information [31] and Granger causality [33]. Unlike TE, mutual in-
286 formation is symmetric; that is, it measures the probabilistic dependence between two processes,
287 but cannot determine the direction of information transfer between them, if there is any [31]. Mea-
288 suring the delayed mutual information between two processes is one way to introduce asymmetry.
289 This takes a step toward inferring whether one process influences another, by measuring shared
290 information between the present state of one process and the past states of another [31]. While
291 the lagged mutual information describes how one process' history predicts the static probabilities
292 of another, the TE measures how one process' history influences the transition probabilities of
293 another. Because of this, the TE is less likely to be confounded by a shared input signal, and
294 is a better measure of stochastic 'driving' [31]. Section 2 of Kaiser and Schreiber (2002) [44]
295 provides a detailed description of the differences between TE and mutual information. Granger
296 causality, on the other hand, is a special case of TE that arises when the stochastic processes are
297 jointly Gaussian-distributed [45]. The TE is thus better suited than Granger causality for making
298 inferences on more general, possibly nonlinear, processes, though this comes at the expense of
299 requiring more data and having no clear way to test statistical significance [45].

300 Convergent cross mapping (CCM) [34] was developed to solve a similar problem as TE, but is
301 based on somewhat different underlying theory. CCM was developed to detect so-called 'causal'

302 relationships in partially stochastic systems with underlying deterministic structure. CCM relies
303 on Takens' theorem [46] to reconstruct candidate manifolds of the underlying dynamical system
304 using lagged observations from two time series. 'Causality' is inferred if nearby points on one
305 reconstructed manifold consistently map to nearby points on the other reconstructed manifold.
306 CCM has been used to provide evidence that temperature and absolute humidity fluctuations
307 drive the timing of global seasonal influenza outbreaks [47], though some controversy surrounds
308 these findings [48, 49]. Nevertheless, it would be interesting to see whether CCM can reveal
309 asymmetric epidemiological interactions between age groups, and to compare its findings with
310 those identified using TE. Lungarella *et al.* (2007) [50] provide more detail on the relationships
311 between various methods that infer asymmetric relationships from time series data. (As an aside,
312 we prefer to avoid the term 'causality' with respect to these methods, despite its frequent use in
313 the literature. Regardless of the vocabulary used, they have successfully detected meaningful
314 relationships between real-world coupled dynamic processes [30, 32, 34, 51, 52, 53]).

315 Despite the apparent well-suitedness of STE for making inferences from ILI data, its epidemio-
316 logical relevance currently remains limited. The calculation of STE requires no prior epidemiolog-
317 ical information whatsoever, which makes its success somewhat surprising. The next-generation
318 matrix [28] is the key object for characterising age-structured, or more generally population-structured,
319 disease transmission dynamics, and yet there is no obvious direct link between STE estimates
320 and the NGM. It is possible that further simulation studies could help identify such a link; even
321 though the STE values seem to bear little mechanistic meaning apart from the relative ordering
322 of age groups that they yield, it is possible that regressing the inferred STE values on an under-
323 lying known NGM could connect the pairwise STE matrix with the NGM under certain conditions.
324 However, it appears unlikely that a simple link exists, especially since STE can say nothing about
325 transmission within a single age group, which is necessary for filling in the diagonal entries of
326 the NGM. STE and related methods such as CCM that do not explicitly incorporate mechanis-
327 tic descriptions of the underlying physical system are unlikely to be able to reveal more than an
328 approximate hierarchy of driving processes. Nevertheless, such a hierarchy can contain valu-
329 able information, especially if developing and fitting a mechanistic model is too demanding to be
330 practicable. Certain extensions to STE could also enhance its relevance for epidemiological in-
331 ference. Local transfer entropy [54] and state-dependent transfer entropy [55], like the contextual
332 STE (see Supplemental Information), are intended to make the TE more flexible and general, by

333 considering how information transfer may change under varying conditions or ‘meta-states’. These
334 extensions may yield better insight into epidemic processes, which are inherently nonlinear and
335 context-dependent, than the more traditional measurements of transfer entropy can provide.

336 Perhaps the most important challenge confronting the TE and related measurements is decid-
337 ing how to measure statistical power and significance. STE calculations rely on a middle level
338 of stochasticity in the underlying stochastic processes; for a deterministic system, the STE will
339 always be exactly zero, while for a stochastic system with too much within-sequence noise, the
340 small-scale variation in amplitudes will likely mask important patterns from which the transfer of
341 information might be inferred. The acceptable range of stochasticity has not been clearly defined.
342 Similarly, it is unclear how best to measure when a difference in STE should be called statistically
343 significant. Though this is recognised as an open and difficult problem [45, 48], it may be possible
344 to make some progress by assuming that the underlying process follows certain epidemiological,
345 or otherwise well-specified, dynamics.

346 5. DISCLAIMER

347 This paper does not necessarily represent the views of the US government or the NIH.

348 6. FUNDING

349 SK was supported by a Gates Cambridge scholarship.

350 REFERENCES

- 351 [1] J. Mossong, N. Hens, M. Jit, P. Beutels, K. Auranen, R. Mikolajczyk, M. Massari, S. Salmaso, G. S. Tomba,
352 J. Wallinga, J. Heijne, M. Sadkowska-Todys, M. Rosinska, and W. J. Edmunds, “Social Contacts and Mixing Pat-
353 terns Relevant to the Spread of Infectious Diseases,” *PLoS Medicine*, vol. 5, p. e74, mar 2008.
- 354 [2] C. Fraser, C. A. Donnelly, S. Cauchemez, W. P. Hanage, M. D. Van Kerkhove, T. D. Hollingsworth, J. Griffin, R. F.
355 Baggaley, H. E. Jenkins, E. J. Lyons, T. Jombart, W. R. Hinsley, N. C. Grassly, F. Balloux, A. C. Ghani, N. M.
356 Ferguson, A. Rambaut, O. G. Pybus, H. Lopez-Gatell, C. M. Alpuche-Aranda, I. B. Chapela, E. P. Zavala, D. M. E.
357 Guevara, F. Checchi, E. Garcia, S. Hugonnet, and C. Roth, “Pandemic potential of a strain of influenza A (H1N1):
358 early findings,” *Science (New York, N.Y.)*, vol. 324, no. 5934, pp. 1557–61, 2009.
- 359 [3] H. Nishiura, C. Castillo-Chavez, M. Safan, and G. Chowell, “Transmission potential of the new influenza A(H1N1)
360 virus and its age-specificity in Japan,” *Eurosurveillance*, vol. 14, no. 22, pp. 1–5, 2009.
- 361 [4] C. J. Worby, S. S. Chaves, J. Wallinga, M. Lipsitch, L. Finelli, and E. Goldstein, “On the relative role of different age
362 groups in influenza epidemics,” *Epidemics*, vol. 13, pp. 10–16, 2015.

- 363 [5] Y. Yang, J. D. Sugimoto, M. E. Halloran, N. E. Basta, D. L. Chao, L. Matrajt, G. Potter, E. Kenah, and I. M. Longini,
364 “The transmissibility and control of pandemic influenza A(H1N1) virus,” *Science*, vol. 326, no. 5953, pp. 729–733,
365 2009.
- 366 [6] J. S. Brownstein, K. P. Kleinman, and K. D. Mandl, “Identifying pediatric age groups for influenza vaccination using
367 a real-time regional surveillance system,” *American Journal of Epidemiology*, vol. 162, no. 7, pp. 686–693, 2005.
- 368 [7] J. Wallinga, P. Teunis, and M. Kretzschmar, “Using data on social contacts to estimate age-specific transmission
369 parameters for respiratory-spread infectious agents,” *American Journal of Epidemiology*, vol. 164, no. 10, pp. 936–
370 944, 2006.
- 371 [8] J. Mossong, N. Hens, M. Jit, P. Beutels, K. Auranen, R. Mikolajczyk, M. Massari, S. Salmaso, G. S. Tomba,
372 J. Wallinga, J. Heijne, M. Sadkowska-Todys, M. Rosinska, and W. J. Edmunds, “Social Contacts and Mixing Pat-
373 terns Relevant to the Spread of Infectious Diseases,” *PLoS Medicine*, vol. 5, p. e74, mar 2008.
- 374 [9] T. Smieszek, M. Balmer, J. Hattendorf, K. W. Axhausen, J. Zinsstag, and R. W. Scholz, “Reconstructing the
375 2003/2004 H3N2 influenza epidemic in Switzerland with a spatially explicit, individual-based model,” *BMC In-
376 fectious Diseases*, vol. 11, no. 1, p. 115, 2011.
- 377 [10] T. Bedford, S. Riley, I. G. Barr, S. Broor, M. Chadha, N. J. Cox, R. S. Daniels, C. P. Gunasekaran, A. C. Hurt,
378 A. Kelso, A. Klimov, N. S. Lewis, X. Li, J. W. McCauley, T. Odagiri, V. Potdar, A. Rambaut, Y. Shu, E. Skepner,
379 D. J. Smith, M. a. Suchard, M. Tashiro, D. Wang, X. Xu, P. Lemey, and C. a. Russell, “Global circulation patterns of
380 seasonal influenza viruses vary with antigenic drift,” *Nature*, vol. 523, no. 7559, pp. 217–20, 2015.
- 381 [11] M. A. Miller, C. Viboud, M. Balinska, and L. Simonsen, “The Signature Features of Influenza Pandemics Implica-
382 tions for Policy,” *New England Journal of Medicine*, vol. 360, no. 25, pp. 2595–2598, 2009.
- 383 [12] I. M. Longini and M. E. Halloran, “Strategy for Distribution of Influenza Vaccine to High-Risk Groups and Children,”
384 *American Journal of Epidemiology*, vol. 161, no. 4, pp. 303–306, 2005.
- 385 [13] S. D. Mylius, T. J. Hagenaars, A. K. Lugnér, and J. Wallinga, “Optimal allocation of pandemic influenza vaccine
386 depends on age, risk and timing,” *Vaccine*, vol. 26, pp. 3742–3749, jul 2008.
- 387 [14] T. A. Reichert, N. Sugaya, D. S. Fedson, W. P. Glezen, L. Simonsen, and M. Tashiro, “The Japanese experience
388 with vaccinating schoolchildren against influenza,” *N Engl J Med*, vol. 344, no. 12, pp. 889–896, 2001.
- 389 [15] V. Gemmetto, A. Barrat, and C. Cattuto, “Mitigation of infectious disease at school: Targeted class closure vs
390 school closure,” *BMC Infectious Diseases*, vol. 14, no. 1, pp. 1–10, 2014.
- 391 [16] G. J. Milne, N. Halder, and J. K. Kelso, “The cost effectiveness of pandemic influenza interventions: a pandemic
392 severity based analysis,” *PloS one*, vol. 8, no. 4, p. e61504, 2013.
- 393 [17] S. Cauchemez, N. M. Ferguson, C. Wachtel, A. Tegnell, G. Saour, B. Duncan, and A. Nicoll, “Closure of schools
394 during an influenza pandemic,” *The Lancet Infectious Diseases*, vol. 9, no. 8, pp. 473–481, 2009.
- 395 [18] C. Viboud, V. Charu, D. Olson, S. Ballesteros, J. Gog, F. Khan, B. Grenfell, and L. Simonsen, “Demonstrating the
396 Use of High-Volume Electronic Medical Claims Data to Monitor Local and Regional Influenza Activity in the US,”
397 *PLoS ONE*, vol. 9, p. e102429, jan 2014.

- 398 [19] Centers for Disease Control and Prevention, “Overview of Influenza Surveillance in the United States,” tech. rep.,
399 Centers for Disease Control and Prevention, 2016.
- 400 [20] J. Ginsberg, M. H. Mohebbi, R. S. Patel, L. Brammer, M. S. Smolinski, and L. Brilliant, “Detecting influenza epi-
401 demics using search engine query data,” *Nature*, vol. 457, pp. 1012–4, feb 2009.
- 402 [21] V. Lampos, T. D. Bie, and N. Cristianini, “Flu Detector - Tracking Epidemics on Twitter,” in *Machine Learning
403 and Knowledge Discovery in Databases* (J. Balcazar, F. Bonchi, M. Sebag, and A. Gionis, eds.), pp. 599–602,
404 Berlin/Heidelberg: Springer-Verlag, 2010.
- 405 [22] D. R. Olson, K. J. Konty, M. Paladini, C. Viboud, and L. Simonsen, “Reassessing Google Flu Trends data for
406 detection of seasonal and pandemic influenza: a comparative epidemiological study at three geographic scales,”
407 *PLoS Computational Biology*, vol. 9, p. e1003256, jan 2013.
- 408 [23] HealthMap, “FluNearYou,” 2017.
- 409 [24] London School of Hygiene and Tropical Medicine, “FluSurvey,” 2017.
- 410 [25] A. J. Adler, K. T. Eames, S. Funk, and W. J. Edmunds, “Incidence and risk factors for influenza-like-illness in the
411 UK: online surveillance using Flusurvey,” *BMC Infectious Diseases*, vol. 14, no. 1, p. 232, 2014.
- 412 [26] D. Perrotta, A. Bella, C. Rizzo, and D. Paolotti, “Participatory online surveillance as a supplementary tool to sentinel
413 doctors for influenza-like illness surveillance in Italy,” *PLoS ONE*, vol. 12, no. 1, pp. 1–15, 2017.
- 414 [27] M. S. Smolinski, A. W. Crawley, K. Baltrusaitis, R. Chunara, J. M. Olsen, O. Wójcik, M. Santillana, A. Nguyen,
415 and J. S. Brownstein, “Flu near you: Crowdsourced symptom reporting spanning 2 influenza seasons,” *American
416 Journal of Public Health*, vol. 105, no. 10, pp. 2124–2130, 2015.
- 417 [28] O. Diekmann, J. A. P. Heesterbeek, and M. G. Roberts, “The construction of next-generation matrices for compart-
418 mental epidemic models,” *Journal of The Royal Society Interface*, vol. 7, no. 47, pp. 873–885, 2010.
- 419 [29] K. Glass, G. N. Mercer, H. Nishiura, E. S. McBryde, and N. G. Becker, “Estimating reproduction numbers for adults
420 and children from case data,” *Journal of The Royal Society Interface*, vol. 8, pp. 1248–1259, sep 2011.
- 421 [30] M. Staniek and K. Lehnertz, “Symbolic Transfer Entropy,” *Phys. Rev. Lett.*, vol. 100, no. April, p. 158101, 2008.
- 422 [31] T. Schreiber, “Measuring Information Transfer,” *Physical Review Letters*, vol. 85, no. 2, p. 19, 2000.
- 423 [32] J. Borge-Holthoefer, N. Perra, B. Goncalves, S. Gonzalez-Bailon, A. Arenas, Y. Moreno, and A. Vespignani, “The
424 dynamics of information-driven coordination phenomena: A transfer entropy analysis,” *Science Advances*, vol. 2,
425 pp. e1501158–e1501158, apr 2016.
- 426 [33] C. W. J. Granger, “Investigating Causal Relations by Econometric Models and Cross-spectral Methods,” *Econo-
427 metrica*, vol. 37, p. 424, aug 1969.
- 428 [34] G. Sugihara, R. May, H. Ye, C.-h. Hsieh, E. Deyle, M. Fogarty, and S. Munch, “Detecting causality in complex
429 ecosystems,” *Science*, vol. 338, pp. 496–500, oct 2012.
- 430 [35] S. V. Scarpino and G. Petri, “On the predictability of infectious disease outbreaks,” *Nature Communications*, vol. 10,
431 no. 1, 2019.
- 432 [36] I. M. Moriyama, R. M. Loy, and A. H. Robb-Smith, “History of the statistical classification of diseases and causes
433 of death,” tech. rep., Centers for Disease Control and Prevention, 2011.

- 434 [37] U.S. Postal Service Office of Inspector General, “The Untold Story of the ZIP Code,” tech. rep., United State Postal
435 Services, 2013.
- 436 [38] D. T. Gillespie, “Exact stochastic simulation of coupled chemical reactions,” *Journal of Physical Chemistry*, vol. 81,
437 no. 25, pp. 2340–2361, 1977.
- 438 [39] M. A. Jhung, D. Swerdlow, S. J. Olsen, D. Jernigan, M. Biggerstaff, L. Kamimoto, K. Kniss, C. Reed, A. Fry,
439 L. Brammer, J. Gindler, W. J. Gregg, J. Bresee, and L. Finelli, “Epidemiology of 2009 pandemic influenza a (H1N1)
440 in the United States,” *Clinical Infectious Diseases*, vol. 52, no. SUPPL. 1, pp. 13–26, 2011.
- 441 [40] W. Yang, M. Lipsitch, and J. Shaman, “Inference of seasonal and pandemic influenza transmission dynamics,”
442 *Proceedings of the National Academy of Sciences*, vol. 112, no. 9, p. 201415012, 2015.
- 443 [41] L. Held, M. Hofmann, M. Höhle, and V. Schmid, “A two-component model for counts of infectious diseases,”
444 *Biostatistics*, vol. 7, no. 3, pp. 422–437, 2006.
- 445 [42] P.-Y. Boëlle, S. Ansart, A. Cori, and A.-J. Valleron, “Transmission parameters of the A/H1N1 (2009) influenza virus
446 pandemic: a review,” *Influenza and Other Respiratory Viruses*, vol. 5, pp. 306–316, sep 2011.
- 447 [43] M. Biggerstaff, M. Jhung, L. Kamimoto, L. Balluz, and L. Finelli, “Self-reported influenza-like illness and receipt of
448 influenza antiviral drugs during the 2009 pandemic, United States, 2009-2010,” *American Journal of Public Health*,
449 vol. 102, no. 10, pp. 2009–2010, 2012.
- 450 [44] A. Kaiser and T. Schreiber, “Information transfer in continuous processes,” *Physica D: Nonlinear Phenomena*,
451 vol. 166, no. 1-2, pp. 43–62, 2002.
- 452 [45] L. Barnett, A. B. Barrett, and A. K. Seth, “Granger causality and transfer entropy Are equivalent for gaussian
453 variables,” *Physical Review Letters*, vol. 103, no. 23, pp. 2–5, 2009.
- 454 [46] F. Takens, “Detecting strange attractors in turbulence,” in *Dynamical Systems and Turbulence* (D. Rand and L.-S.
455 Young, eds.), pp. 366–381, Springer-Verlag, 1981.
- 456 [47] E. R. Deyle, M. C. Maher, R. D. Hernandez, S. Basu, and G. Sugihara, “Global environmental drivers of influenza.,”
457 *Proceedings of the National Academy of Sciences of the United States of America*, vol. 113, no. 46, p. 201607747,
458 2016.
- 459 [48] E. B. Baskerville and S. Cobey, “Does influenza drive absolute humidity?,” *Proceedings of the National Academy
460 of Sciences*, vol. 114, no. 12, pp. E2270–E2271, 2017.
- 461 [49] G. Sugihara, E. R. Deyle, and H. Ye, “Reply to Baskerville and Cobey: Misconceptions about causation with syn-
462 chrony and seasonal drivers.,” *Proceedings of the National Academy of Sciences of the United States of America*,
463 vol. 114, no. 12, pp. E2272–E2274, 2017.
- 464 [50] M. Lungarella, K. Ishiguro, Y. Kuniyoshi, and N. Otsu, “Methods for Quantifying the Causal Structure of Bivariate
465 Time Series,” *International Journal of Bifurcation and Chaos*, vol. 17, no. 03, pp. 903–921, 2007.
- 466 [51] M. Kamiński, M. Ding, W. A. Truccolo, and S. L. Bressler, “Evaluating causal relations in neural systems: Granger
467 causality, directed transfer function and statistical assessment of significance,” *Biological Cybernetics*, vol. 85,
468 no. 2, pp. 145–157, 2001.

- 469 [52] J. Pahle, A. K. Green, C. J. Dixon, and U. Kummer, "Information transfer in signaling pathways: a study using
470 coupled simulated and experimental data.," *BMC bioinformatics*, vol. 9, p. 139, 2008.
- 471 [53] G. V. Steeg and A. Galstyan, "Information Transfer in Social Media," *Entropy*, vol. 90292, no. 1, pp. 1–8, 2011.
- 472 [54] J. T. Lizier, M. Prokopenko, and A. Y. Zomaya, "Local information transfer as a spatiotemporal filter for complex
473 systems," *Physical Review E - Statistical, Nonlinear, and Soft Matter Physics*, vol. 77, no. 2, pp. 1–11, 2008.
- 474 [55] P. L. Williams and R. D. Beer, "Generalized measures of information transfer," *arXiv:1102.1507*, pp. 1–6, 2011.